Double Intelligent Reflecting Surface for Secure Transmission With Inter-Surface Signal Reflection

Limeng Dong, Hui-Ming Wang, *Senior Member, IEEE*, Jiale Bai, and Haitao Xiao

***Abstract*—In this correspondence, we use double intelligent reflecting surface (IRS) assisted design to enhance the secrecy performance of wireless transmission. Different from the existing studies in the literature, the inter-surface signal reflection is considered in this work, which makes the formulated secrecy rate (SR) optimization problem difficult to tackle. In particular, to solve this problem, we propose a product Riemmanian manifold (PRM) based alternating optimization (AO) algorithm to jointly optimize the beamformer at transmitter as well as phase shift coefficients at double IRS, in which the PRM optimization algorithm is applied to optimize the phase shift coefficients at both IRSs simultaneously. Simulation results show that the proposed algorithm greatly enhance the SR compared with the existing benchmark schemes. And compared with conventional semi-definite relaxation based AO algorithm, the proposed PRM based AO algorithm can achieve much lower computational complexity as well as faster speed of convergence.**

***Index Terms*—Alternating optimization, intelligent reflecting surface, inter-surface signal reflection, product Riemmanian manifold, secrecy rate.**

I. Introduction

Intelligent reflecting surface (IRS) has drawn wide attentions in academic and industry due to its flexible and energy-efficient properties. IRS is a software-controlled metasurface consisting of low complexity passive reflecting elements. These elements are able to induce certain phase shifts for the incident electromagnetic signal waves with very low power consumptions so that the quality of user's communication can be greatly improved [1]. Motivated by these advantages, IRS has been applied to increase the achievable rate of users in multi-antenna channels [2], [3]. Later, IRS is combined with physical layer security to enhance the user's secrecy rate (SR) in wiretap channels (WTCs), such as multi-input single-output (MISO) [5]–[6], and multi-input multi-output WTC [7], [8]. All these studies indicate that the IRS-assisted design greatly help enhancing the performance in secure and non-secure communication.

Recently, the study of multi-IRS assisted design for enhancing the non-secure and secure wireless transmission have also been established [9]–[11]. In [9], a double-IRS assisted multi-user uplink channel has been considered, and numerical algorithm is proposed to maximize the minimum achievable rate among all users. In [10], [11], multi-IRS assisted design is also applied to enhance the secure communication of users. And numerical algorithms are also proposed to maximize the SR based on full channel state information (CSI) and imperfect CSI of eavesdropper. In addition, channel estimation for the double IRS assisted model has also been investigated in [12].

Manuscript received December 7, 2020; revised January 22, 2021; accepted February 21, 2021. Date of publication February 25, 2021; date of current version April 2, 2021. This work was supported in part by the National Natural Science Foundation of China under Grants 61941118 and 61941105, and in part by the Innovation Team Research Fund of Shaanxi Province under Grant 2019TD-013. The review of this article was coordinated by Dr. B. Di. *(Corresponding author: Hui-Ming Wang.)*

The authors are with the School of Information and Communications Engineering, Xi'an Jiaotong University, Xi'an 710049, China, and also with the Ministry of Education Key Laboratory for Intelligent Networks and Network Security, Xi'an Jiaotong University, Xi'an 710049, China (e-mail: dlm_nwpu@hotmail.com; xjbswhm@gmail.com; bjl19970954@stu.xjtu.edu.cn; xht8015949@xjtu.edu.cn).

Digital Object Identifier 10.1109/TVT.2021.3062059

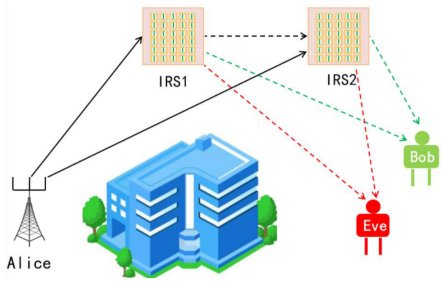

Fig. 1. A block diagram of Double IRS-assisted MISO WTC.

However, a significant drawback in the current study for secure multi-IRS assisted channels [10], [11] is that the inter-surface signal reflection (I-SSR) has been ignored so that no cooperation exists among all the IRSs. In particular, the I-SSR should be considered since it provides new path for wireless transmission. As a consequence, it brings new opportunities for achieving larger SR performance. Note that although the system model illustrated in [9] considers the I-SSR, it is unrelated with security issues. Hence, in this correspondence, we study a secure double IRS assisted channel with I-SSR, and aim at maximizing the SR at user. To tackle the non-convex problem, we apply alternating optimization (AO) algorithm to jointly optimize the beamformer (BF) at transmitter and phase shift coefficients (PSCs) at double IRS respectively. And in particular, a product Riemmanian manifold (PRM) algorithm is established to optimize the PSCs simultaneously at both IRSs given BF in AO algorithm. To the best of our knowledge, this algorithm has never been used to optimize the PSCs in multi-IRS assisted wireless communications. Furthermore, to make a performance comparison with PRM, we also propose semi-definite relaxation (SDR) method to optimize the PSCs at each IRS alternatively. Simulation results have been shown that the proposed PRM based AO algorithm has very close performance on enhancing the SR but with significantly faster speed of convergence compared with the SDR based AO algorithm.

Notations: $\mathbf{A}^T$, $\mathbf{A}^*$ and $\mathbf{A}^H$ denote transpose, conjugate and Hermitian conjugate of $\mathbf{A}$ respectively; $tr(\mathbf{A})$ is the trace of $\mathbf{A}$; $\odot$ denotes Hadamard product; $Re\{\mathbf{A}\}$ denotes the real elements in $\mathbf{A}$; $diag(\mathbf{a})$ is to transform vector $\mathbf{a}$ to diagonal matrix with diagonal elements in $\mathbf{a}$; $\mathbf{u}_{max}(\mathbf{A})$ denotes the eigenvector corresponding to the largest eigenvalue of $\mathbf{A}$; $\mathbf{a}(i)$ denotes the i-th entry in $\mathbf{a}$; $|\mathbf{a}|$ denotes the Euclidean norm of $\mathbf{a}$; $\langle \mathbf{a}, \mathbf{b} \rangle = Re\{\mathbf{a}^H \mathbf{b}\}$.

II. Channel Model and Problem Formulation

Considering a double IRS assisted MISO WTC model shown in Fig. 1, in which IRS1, IRS2, a transmitter (Alice), receiver (Bob) as well as an eavesdropper (Eve) are included. Alice are equipped with m antennas, IRS1 and IRS2 are equipped with n_1 and n_2 reflecting elements respectively, and both Bob and Eve are equipped with single antenna. We assume that these nodes are deployed in a city's hot spot, and the direct communication links of Alice-Bob (Eve) is blocked by buildings. To help Alice's transmission, one IRS is deployed close to

Alice, the other one is deployed close to Bob so as to create virtual line-of-sight links between Alice and Bob,[1] and there exists I-SSR between IRS1 and IRS2. To help Alice enhancing the secrecy performance, the task of double IRS in this model is to cooperatively adjust the phase shift of the incident signals via the reflecting elements so as to enhance the achievable SR at Bob. To the best of our knowledge, the study of this proposed system model has never been investigated in the current literatures.

Based on this setting, the received signals at Bob $\mathbf{y}_B$ and Eve $\mathbf{y}_E$ can be expressed as $\mathbf{y}_i = \mathbf{h}_{Ii1}^T diag(\mathbf{s}_1^*)\mathbf{H}_{AI1}\mathbf{x} + \mathbf{h}_{Ii2}^T diag(\mathbf{s}_2^*)\mathbf{H}_{AI2}\mathbf{x} + \mathbf{h}_{Ii2}^T diag(\mathbf{s}_2^*)\mathbf{H}_I diag(\mathbf{s}_1^*)\mathbf{H}_{AI1}\mathbf{x} + \xi_i, i \in \{B, E\}$, where $\mathbf{x} = \mathbf{w}s$ is the transmitted signal, s is the confidential message with zero mean and unit variance, $\mathbf{w}$ is the BF, $\mathbf{H}_{AI1}$, $\mathbf{H}_{AI2}$, $\mathbf{H}_I$, $\mathbf{h}_{IB1}$, $\mathbf{h}_{IE1}$, $\mathbf{h}_{IB2}$, $\mathbf{h}_{IE2}$ are the channels representing the links of Alice-IRS1, Alice-IRS2, IRS1-IRS2, IRS1-Bob, IRS1-Eve, IRS2-Bob, IRS2-Eve respectively, $\mathbf{s}_1 \in \mathbb{C}^{n_1}$ and $\mathbf{s}_2 \in \mathbb{C}^{n_2}$, $\mathbf{s}_1(l)^*$ and $\mathbf{s}_2(j)^*$ are the PSCs of the l-th and j-th reflecting elements at IRS1 and IRS2 respectively, ξ_i is the noise following zero mean and variance σ_i^2. We assume that full CSI of all the channel links are available at Alice, this can be realized since Eve is just other user in the system and it also share its CSI with Alice but is untrusted by Bob [4]. And the existing method in [12] can be applied to estimate each channels.[2]

In order to express the function conveniently, in the rest correspondence, we mix the noise term with the channels together, i.e., $\mathbf{h}_{IB1(2)}/\sigma_B$ and $\mathbf{h}_{IE1(2)}/\sigma_E$ are represented as $\mathbf{h}_{IB1(2)}$, $\mathbf{h}_{IE1(2)}$ respectively. Therefore, for $l = 1, 2, \ldots, n_1$, $j = 1, 2, \ldots, n_2$, we formulate the achievable SR optimization problem as

$$\text{(P1)} \max_{\mathbf{w},\mathbf{s}_1,\mathbf{s}_2} \log_2(1 + |\mathbf{h}_B^T\mathbf{w}|^2) - \log_2(1 + |\mathbf{h}_E^T\mathbf{w}|^2)$$
$$\text{s.t. } |\mathbf{w}|^2 \le P, |\mathbf{s}_1(l)| = 1, |\mathbf{s}_2(j)| = 1, \forall l, j$$

where $\mathbf{h}_i = (\mathbf{h}_{Ii1}^T diag(\mathbf{s}_1^*)\mathbf{H}_{AI1} + \mathbf{h}_{Ii2}^T diag(\mathbf{s}_2^*)\mathbf{H}_{AI2} + \mathbf{h}_{Ii2}^T diag(\mathbf{s}_2^*)\mathbf{H}_I diag(\mathbf{s}_1^*)\mathbf{H}_{AI1})^T, i \in \{B, E\}$, P is the total transmit power budget at Alice, $|\mathbf{s}_1(l)| = 1, |\mathbf{s}_2(j)| = 1$ are the unit modulus constraints (UMCs) which guarantees that IRS is only capable of adjusting the phase of incident signals without changing the amplitude. P1 is a non-convex problem due to non-convex objective function with respect to $\mathbf{w}$, $\mathbf{s}_1$, $\mathbf{s}_2$ and non-convex UMCs.

Remark 1: Without the I-SSR channel $\mathbf{H}_I$, the double IRS design is just equivalent to a single IRS so that the objective function can be manipulated in which the variable $\mathbf{s}_1$ and $\mathbf{s}_2$ are merged into a single variable as in [10], [11], and the existing solutions [4], [5] can be directly applied to solve this problem. However, since $\mathbf{H}_I$ is considered in this work, $\mathbf{s}_1$ and $\mathbf{s}_2$ cannot be merged as a single variable due to the extra term $\mathbf{h}_{Ii2}^T diag(\mathbf{s}_2^*)\mathbf{H}_I diag(\mathbf{s}_1^*)\mathbf{H}_{AI1}\mathbf{x}$ in $\mathbf{y}_i$, thereby significantly increasing the difficulty for optimization.

III. Alternating Optimization Algorithm

To solve the non-convex P1, in this section, we propose AO algorithm to optimize $\mathbf{w}$, $\mathbf{s}_1$ and $\mathbf{s}_2$. Specifically, given fixed $\mathbf{s}_1$ and $\mathbf{s}_2$, $\mathbf{h}_B$ and $\mathbf{h}_E$ are fixed so that P1 reduces to a MISO secrecy capacity optimization problem. Therefore, a closed-form solution of optimal $\mathbf{w}$ can be obtained as [4], [5]:

$$\mathbf{w} = \sqrt{P}\mathbf{u}_{max}((\mathbf{B} + P^{-1}\mathbf{I})^{-1}(\mathbf{A} + P^{-1}\mathbf{I})) \quad (1)$$

where $\mathbf{A} = \mathbf{h}_B^*\mathbf{h}_B^T$ and $\mathbf{B} = \mathbf{h}_E^*\mathbf{h}_E^T$. When $\mathbf{w}$ is fixed, the sub-problem of optimizing the PSCs can be simplified as $\text{(P2)} \max_{\mathbf{s}_1,\mathbf{s}_2} (1 + |\mathbf{h}_B^T\mathbf{w}|^2)(1 + |\mathbf{h}_E^T\mathbf{w}|^2)^{-1}$ s.t. $|\mathbf{s}_1(l)| = 1, |\mathbf{s}_2(j)| = 1, \ \forall l, j$. P2 is a non-convex problem due to the complicated objective function as well as UMCs. In the following, we firstly propose a PRM algorithm to simultaneously optimize $\mathbf{s}_1$ and $\mathbf{s}_2$. And then we propose another SDR method to optimize $\mathbf{s}_1$ and $\mathbf{s}_2$ alternatively by fixing one of them as a constant.

A. PRM Algorithm

In this subsection, we propose an iterative PRM algorithm to optimize $\mathbf{s}_1$, $\mathbf{s}_2$ simultaneously. Specifically, let $\mathcal{M}_1 = \{\mathbf{s}_1 : |\mathbf{s}_1(1)| = |\mathbf{s}_1(2)| = \cdots = |\mathbf{s}_1(n_1)| = 1\}$, $\mathcal{M}_2 = \{\mathbf{s}_2 : |\mathbf{s}_2(1)| = |\mathbf{s}_2(2)| = \cdots = |\mathbf{s}_2(n_2)| = 1\}$, as can be seen, the feasible set $\mathcal{M}_1$ and $\mathcal{M}_2$ are complex circle manifolds of dimension n_1 and n_2 respectively. Then, we define the set $\mathcal{M} = \mathcal{M}_1 \times \mathcal{M}_2$ as the set of pairs $(\mathbf{s}_1, \mathbf{s}_2)$, where $\mathbf{s}_1 \in \mathcal{M}_1$, $\mathbf{s}_2 \in \mathcal{M}_2$, which is also called the product of the manifolds $\mathcal{M}_1$ and $\mathcal{M}_2$ [14]. Then we can re-express P2 as

$$\text{(P3)} \min_{(\mathbf{s}_1,\mathbf{s}_2)\in\mathcal{M}} g(\mathbf{s}_1, \mathbf{s}_2) = (1 + |\mathbf{h}_E^T\mathbf{w}|^2)(1 + |\mathbf{h}_B^T\mathbf{w}|^2)^{-1}$$

The key idea of PRM algorithm is to search for a sequence of $(\mathbf{s}_{1,k}, \mathbf{s}_{2,k}), k = 0, 1, ..$ in the product manifolds $\mathcal{M}$ such that $g(\mathbf{s}_{1,k}, \mathbf{s}_{2,k})$ is monotonically non-increasing with iteration k. During each iteration, the search direction at point $(\mathbf{s}_{1,k}, \mathbf{s}_{2,k})$ in the current tangent space (which will be described later) as well as the step size used for updating $(\mathbf{s}_{1,k}, \mathbf{s}_{2,k})$ in the next iteration can be properly adjusted. As the convergence is reached, the solution returned by PRM algorithm is an Riemannian zero gradient point solution, which can be as a suboptimal solution of P3. The main advantages of this algorithm is that it can directly handle this complicate problem with the non-convex UMCs (without any approximation) by the theory of manifold optimization [14], [15], and it requires a lower computational complexity compared with conventional SDR method.

To develop the PRM algorithm, we firstly give the tangent space of manifold $\mathcal{M}$ at the point $(\mathbf{s}_1, \mathbf{s}_2)$. For any point $\mathbf{s}_{1(2)} \in \mathcal{M}_{1(2)}$, the tangent space is composed of all the tangent vectors $\mathbf{z}_{1(2)}$ that tangentially pass through $\mathbf{s}_{1(2)}$. Since the manifold $\mathcal{M}$ is a product manifold, the corresponding tangent space $T_{(\mathbf{s}_1,\mathbf{s}_2)}\mathcal{M}$ can be decomposed as a product of two tangent spaces $T_{(\mathbf{s}_1,\mathbf{s}_2)}\mathcal{M} = T_{\mathbf{s}_1}\mathcal{M}_1 \times T_{\mathbf{s}_2}\mathcal{M}_2$ where the tangent space $T_{\mathbf{s}_1}\mathcal{M}_1$ at point $\mathbf{s}_1 \in \mathcal{M}_1$ and $T_{\mathbf{s}_2}\mathcal{M}_2$ at point $\mathbf{s}_2 \in \mathcal{M}_2$ are defined as $T_{\mathbf{s}_1}\mathcal{M}_1 = \{\mathbf{z}_1 \in \mathbb{C}^{n_1} : Re\{\mathbf{z}_1 \odot \mathbf{s}_1^*\} = \mathbf{0}\}$, $T_{\mathbf{s}_2}\mathcal{M}_2 = \{\mathbf{z}_2 \in \mathbb{C}^{n_2} : Re\{\mathbf{z}_2 \odot \mathbf{s}_2^*\} = \mathbf{0}\}$ respectively where $\mathbf{z}_1$ and $\mathbf{z}_2$ are tangent vectors at point $\mathbf{s}_1$ and $\mathbf{s}_2$ respectively.

With the concept of tangent space, the next key part in PRM algorithm is the Riemannian gradient, which is one tangent direction with the steepest decrease of the objective function among all the tangent vectors in the tangent space. Since the complex circle manifold $\mathcal{M}_{1(2)}$ is an Riemannian submanifold of $\mathbb{C}^{n_{1(2)}}$, the Riemannian gradient $grad_{\mathbf{s}_{1(2)}}g$ at point $\mathbf{s}_{1(2)}$ is the orthogonal projection of the Euclidean gradient $Grad_{\mathbf{s}_{1(2)}}g$ onto tangent space $T_{\mathbf{s}_{1(2)}}\mathcal{M}_{1(2)}$. Therefore, denote k as the iteration index in PRM algorithm, the Riemannian gradient of $g(\mathbf{s}_{1,k}, \mathbf{s}_{2,k})$ at $\mathbf{s}_{1,k}$ and $\mathbf{s}_{2,k}$ can be expressed as $grad_{\mathbf{s}_{1(2),k}}g = Grad_{\mathbf{s}_{1(2),k}}g - Re\{Grad_{\mathbf{s}_{1(2),k}}g \odot \mathbf{s}_{1,k}^*\} \odot \mathbf{s}_{1(2),k}$, where for $i \in \{B, E\}$, $Grad_{\mathbf{s}_{1,k}}g = [2(\mathbf{t}_E\mathbf{t}_E^H\mathbf{s}_{1,k} + \mathbf{t}_E t_E^*)(1 + |\mathbf{s}_{1,k}^H\mathbf{t}_B + t_B|^2) -$

[1]We remark that although our system model does not consider the direct link of Alice-Bob (Eve), our proposed numerical solutions for enhancing the SR also can be applied to the general case where these direct links exist.

[2]The study of enhancing SR under imperfect Eve's CSI will be considered as our future directions. Note that in our previous work [6] an artificial noise aided approach is proposed to enhance the SR under no Eve's CSI and single IRS design, which can also be applied to the double IRS design in this work.

Algorithm 1: *(PRM Algorithm).*

Require: $\epsilon_1 > 0$, $c, \tau \in (0,1)$, initial point $\mathbf{s}_{1,0}$, $\mathbf{s}_{2,0}$
1. Set $k=0$, $\beta_{1(2),0}=0$, compute $d_{1(2),0} = -grad_{\mathbf{s}_{1(2),0}} g$.
repeat (conjugate gradient descent search)
2. Set $\alpha = 1$.
repeat (backtracking line search algorithm)
3. Set $\alpha = \tau\alpha$, and $\mathbf{s}_{1(2),k+1} = \mathbf{s}_{1(2),k} + \alpha d_{1(2),k}$.
until $g(\mathbf{s}_{1,k}, \mathbf{s}_{2,k}) - g(R(\mathbf{s}_{1,k+1}), R(\mathbf{s}_{2,k+1})) \geq c\tau(\langle -grad_{\mathbf{s}_{1,k}} g, d_{1,k}\rangle + \langle -grad_{\mathbf{s}_{2,k}} g, d_{2,k}\rangle)$
4. Set $\mathbf{s}_{1(2),k+1} = R(\mathbf{s}_{1(2),k+1})$, and compute $grad_{\mathbf{s}_{1(2),k+1}} g$ given $\mathbf{s}_{1(2),k+1}$.
5. If $|[grad_{\mathbf{s}_{1,k+1}} g^T, grad_{\mathbf{s}_{2,k+1}} g^T]^T| \leq \epsilon_1$, stop the algorithm, else go to step 6.
6. Compute Riemannian gradient $grad_{\mathbf{s}_{1(2),k+1}} g$ at point $\mathbf{s}_{1(2),k+1}$, then provide vector transport $T_{\mathbf{s}_{1(2),k} \to \mathbf{s}_{1(2),k+1}}$, and then choose the Polak-Ribière parameter $\beta_{1(2),k+1}$.
7. Compute search direction $d_{1(2),k+1}$ at point $\mathbf{s}_{1(2),k+1}$, and set $k = k+1$.
until $|[grad_{\mathbf{s}_{1,k}} g^T, grad_{\mathbf{s}_{2,k}} g^T]^T| \leq \epsilon_1$

$2(\mathbf{t}_B \mathbf{t}_B^H \mathbf{s}_{1,k} + \mathbf{t}_B t_B^*)(1+|\mathbf{s}_{1,k}^H \mathbf{t}_E + t_E|^2)]/(1+|\mathbf{s}_{1,k}^H \mathbf{t}_B + t_B|^2)^2$, $Grad_{\mathbf{s}_{2,k}} g = [2(\mathbf{r}_E \mathbf{r}_E^H \mathbf{s}_{2,k} + \mathbf{r}_E r_E^*)(1+|\mathbf{s}_{2,k}^H \mathbf{r}_B + r_B|^2) - 2(\mathbf{r}_B \mathbf{r}_B^H \mathbf{s}_{2,k} + \mathbf{r}_B r_B^*)(1+|\mathbf{s}_{2,k}^H \mathbf{r}_E + r_E|^2)]/(1+|\mathbf{s}_{2,k}^H \mathbf{r}_B + r_B|^2)^2$, $\mathbf{t}_i = (diag(\mathbf{h}_{Ii1})\mathbf{H}_{AI1} + diag((\mathbf{h}_{Ii2}^T diag(\mathbf{s}_2^*)\mathbf{H}_I)^T)\mathbf{H}_{AI1})\mathbf{w}$, $\mathbf{r}_i = (diag(\mathbf{h}_{Ii2})\mathbf{H}_{AI2} + diag(\mathbf{h}_{Ii2}^T)\mathbf{H}_I diag(\mathbf{s}_1^*)\mathbf{H}_{AI1})\mathbf{w}$, $t_i = \mathbf{h}_{Ii2}^T diag(\mathbf{s}_2^*)\mathbf{H}_{AI2}\mathbf{w}$, $r_i = \mathbf{h}_{Ii1}^T diag(\mathbf{s}_1^*)\mathbf{H}_{AI1}\mathbf{w}$.

After obtaining the Riemannian gradient, the search direction $d_{1,k}$, $d_{2,k}$ at $\mathbf{s}_{1,k}$, $\mathbf{s}_{2,k}$ can be updated as $d_{1(2),k} = -grad_{\mathbf{s}_{1(2),k}} + \beta_{1(2),k} T_{\mathbf{s}_{1(2),k-1} \to \mathbf{s}_{1(2),k}}(d_{1(2),k-1})$, where $\beta_{1(2),k}$ is Polak-Ribière parameter defined as [14]

$$\beta_{1(2),k} = \frac{\langle grad_{\mathbf{s}_{1(2),k}}, grad_{\mathbf{s}_{1(2),k}} - grad_{\mathbf{s}_{1(2),k-1}} \rangle}{\langle grad_{\mathbf{s}_{1(2),k-1}}, grad_{\mathbf{s}_{1(2),k-1}} \rangle}$$

and where $T_{\mathbf{s}_{1(2),k-1} \to \mathbf{s}_{1(2),k}}(d_{1(2),k-1}) = d_{1(2),k-1} - Re\{d_{1(2),k-1} \odot \mathbf{s}_{1(2),k}^*\} \odot \mathbf{s}_{1(2),k}$ is the vector transport[3] for manifold $\mathcal{M}_{1(2)}$.

With $d_{1(2),k}$, then $\mathbf{s}_{1(2),k}$ can be updated as $\mathbf{s}_{1(2),k+1} = \mathbf{s}_{1(2),k} + \alpha d_{1(2),k}$ where α is the step size which can be found using backtracking line search algorithm [14]. Note that the new updated $\mathbf{s}_{1(2),k+1}$ may not satisfy the UMCs, hence, an retraction operation is needed during each iteration of backtracking line search defined as $R(\mathbf{s}_{1(2),k+1}) = \mathbf{s}_{1(2),k+1}/|\mathbf{s}_{1(2),k+1}|$ so that the norm of each entry of $\mathbf{s}_{1(2)}$ is one.

We summarize the PRM algorithm as Algorithm 1. In this algorithm, c is the percentage of the decrease in the value of $g(\mathbf{s}_1, \mathbf{s}_2)$ one is willing to accept in the backtracking line search, τ are the parameters controlling the reduction in step size α, ϵ_1 is the target accuracy for the convergence of Riemannian gradient. As the algorithm starts, when $k=0$, we firstly set $-grad_{\mathbf{s}_{1,k}}$ and $-grad_{\mathbf{s}_{2,k}}$ as the initial search direction at $\mathbf{s}_{1,k}$ and $\mathbf{s}_{2,k}$ respectively, and then obtain the step size α via backtracking line search. If the target accuracy is met, then the algorithm stops, else go to step 6 to compute the Riemannian gradient, vector transport under current point as well as Polak-Ribière parameter for the next iteration. Since $g(\mathbf{s}_1, \mathbf{s}_2)$ is bounded on $\mathcal{M}$ and it has a Lipschitz gradient with constant L that is independent with $\mathbf{s}_1$ and $\mathbf{s}_2$, the proposed PRM in combination with backtracking line search algorithm guarantees that the sequence $\{g(\mathbf{s}_{1,k}, \mathbf{s}_{2,k})\}_{k=0}^{\infty}$ is monotonically non-increasing and finally converges to a Riemmannian zero gradient point [15]. As can be seen, the main computational complexity of this algorithm only lies on computing the Euclidean gradient $Grad_{\mathbf{s}_{1(2)}} g$, which is about $\mathcal{O}(n_1^2 + n_2^2)$.

[3]We remark that $d_{1(2),k-1}$ and $d_{1(2),k}$ in the manifold optimization lie in two different tangent spaces $T_{\mathbf{s}_{1(2),k-1}}$ and $T_{\mathbf{s}_{1(2),k}}$. Hence, vector transport is used to map a tangent vector from one tangent space to the other.

B. SDR Method

To make a performance comparison with PRM, in this subsection, we apply SDR method to optimize the PSCs. Since the objective function in P2 is of a complicated structure due to the existence of $\mathbf{H}_I$, it is difficult to simultaneously optimize $\mathbf{s}_1$ and $\mathbf{s}_2$ via SDR as in PRM algorithm. Therefore, we alternatively optimize $\mathbf{s}_1$ and $\mathbf{s}_2$ by fixing one of the other as a constant. When $\mathbf{w}$ and $\mathbf{s}_2$ are fixed, the sub-problem of optimizing $\mathbf{s}_1$ can be expressed as:

$$\text{(P4)} \max_{\mathbf{s}_1} (1+|\mathbf{s}_1^H \mathbf{t}_B + t_B|^2)(1+|\mathbf{s}_1^H \mathbf{t}_E + t_E|^2)^{-1}$$
$$\text{s.t. } |\mathbf{s}_1(l)| = 1, \forall l.$$

Based on the key idea of SDR, let $\tilde{\mathbf{s}}_1 = [\mathbf{s}_1^T, 1]^T$, $\mathbf{S}_1 = \tilde{\mathbf{s}}_1 \tilde{\mathbf{s}}_1^H$, using Charnes-Cooper transformation, P4 transforms to:

$$\text{(P5)} \max_{\mathbf{X} \geq \mathbf{0}, \mu \geq 0} \quad tr(\mathbf{T}_B \mathbf{X}) + \mu \text{ s.t.}$$
$$tr(\mathbf{T}_E \mathbf{X}) + \mu = 1, tr(\mathbf{E}_d \mathbf{X}) = \mu, d = 1, 2, \ldots, n_1 + 1, \quad (2)$$

where $\mathbf{X} = \mu \mathbf{S}_1$, $\mu = 1/(tr(\mathbf{T}_E \mathbf{S}_1) + 1)$,

$$\mathbf{T}_B = \begin{bmatrix} \mathbf{t}_B \mathbf{t}_B^H & \mathbf{t}_B t_B^* \\ t_B \mathbf{t}_B^H & |t_B|^2 \end{bmatrix}, \mathbf{T}_E = \begin{bmatrix} \mathbf{t}_E \mathbf{t}_E^H & \mathbf{t}_E t_E^* \\ t_E \mathbf{t}_E^H & |t_E|^2 \end{bmatrix},$$

$\mathbf{E}_d$ is a diagonal matrix in which only the d-th diagonal entry is one and the rest entries are all zero. P5 is convex and can be directly optimized via CVX. Since the rank-1 constraint of $\mathbf{X}$ is omitted here, the solution may not be of rank-1 so that the original $\mathbf{s}_1$ cannot be recovered. Therefore, inspired by [13], we use the sequential rank-one constraint relaxation (SROCR) algorithm to recover the global optimal rank-1 solution of $\mathbf{X}$ in (P5). The key idea of SROCR is to relax the rank-1 constraint by adding relaxation parameters, and then gradually optimize the relaxed problem so that the largest eigenvector of $\mathbf{X}_k$ in the k-th iteration is gradually projected onto an updated direction $\mathbf{u}_{max}(\mathbf{X}_{k-1})$ until all the power lies in a one-dimensional subspace. As the algorithm converges, the solution $\mathbf{X}^{(k)}$ is the global optimal rank-1 solution so that the optimal $\mathbf{s}_1$ for P4 can be obtained. The detailed steps of this algorithm can be found in [13].

Identically, when solving $\mathbf{s}_2$ for IRS2 given $\mathbf{s}_1$ and $\mathbf{w}$, a similar optimization sub-problem of $\mathbf{s}_2$ can be formulated as $\max_{\mathbf{s}_2} (1+|\mathbf{s}_2^H \mathbf{r}_B + r_B|^2)(1+|\mathbf{s}_2^H \mathbf{r}_E + r_E|^2)^{-1}$, s.t. $|\mathbf{s}_2(j)| = 1, \forall j$. Using SDR method with SROCR, a global optimal solution of $\mathbf{s}_2$ for P6 given $\mathbf{s}_1$ and $\mathbf{w}$ can be obtained as well. Compared with PRM algorithm, SDR method cannot optimize $\mathbf{s}_1$ and $\mathbf{s}_2$ simultaneously in P2, and it requires higher computational complexity with $\mathcal{O}((n_1+1)^3 + (n_2+1)^3)$.

C. Summary of the AO Algorithm

Finally, we summarize the AO algorithm as Algorithm 2, C_k is the value of objective function in P1 in the k-th iteration. Since $\mathbf{w}$ and $\mathbf{s}_1$, $\mathbf{s}_2$ are all bounded by the constraints, the AO algorithms is guaranteed to have a monotonic convergence. If $\mathbf{s}_1$, $\mathbf{s}_2$ are optimized using PRM algorithm, the converged point returned by AO algorithm is a limit

Algorithm 2: *(AO Algorithm for Solving P1).*

Require: Starting point of BF, PSCs, $\epsilon_2 > 0$.
1. Set $k = 0$, compute C_k.
repeat (AO algorithm)
2. Set $k = k + 1$, optimize BF given PSCs via (1).
3. Optimize PSCs given BF via Algorithm 1 or SDR.
4. Compute C_{k+1}.
until $|C_{k+1} - C_k| \leq \epsilon_2$

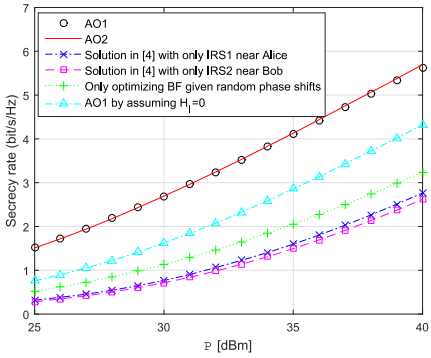

Fig. 2. SR performance returned by the proposed AO1 and AO2 and other benchmark schemes, $m = 3, n_1 = n_2 = 4$.

point solution. If they are optimized using SDR, the converged point is a Karush-Khun-Tucker (KKT) point solution.[4]

IV. Simulation Results

To validate the performance of our proposed algorithm for this double IRS assisted design, simulation results have been carried out in this section. All the channels are assumed to be independent Rayleigh fading, and each channel vector (matrix) is formulated as the product of large scale fading and small scale fading. The small scale fading is randomly generated with complex Gaussian random variables with zero mean, unit variance in each entry of the channel vector (matrix). For the large scale fading, we follow [4] and set -30 dBm as the pass loss at the reference distance 1 m, and the path loss exponents are set as 2.5 for all the communication links. The noise power σ_i^2 is set as -100 dBm. For the location of each node, we consider a three dimensional coordinate space, and let Alice, Bob to be fixed at the coordinates (0,0,0), (100,0,0) respectively. We deploy IRS1 at $(20, -10, 30)$ which is located near Alice and IRS2 at $(80, -10, 30)$ which is located near Bob. And we set Eve to be randomly located in a circle with Bob as the center and a radius of 50. In Algorithm 1 and 2, $\epsilon_1 = \epsilon_2 = 10^{-3}$, and $c = 0.3$, $\tau = 0.5$. In the SDR method, the target accuracy of SROCR algorithm for recovering rank-1 solution is also 10^{-3}. To simplify the description of algorithms, in the rest of correspondence, we denote the proposed PRM based AO algorithm as AO1, and the SDR based AO algorithm as AO2. For both AO1 and AO2, we set the starting point as $\mathbf{w} = \mathbf{0}$ and $\mathbf{s}_1(l) = 1, \mathbf{s}_2(j) = 1, \forall l, j$.

Fig. 2 shows the performance of SR versus P, the results are averaged over 500 random channel realizations. We propose four benchmark schemes to compare their performance with the proposed algorithms: 1) only optimizing $\mathbf{w}$ given random PSCs for double IRS; 2) solutions in [4] with only IRS1 near Alice; 3) solutions in [4] with only IRS2 near Bob; 4) proposed algorithm by ignoring the I-SSR channel $\mathbf{H}_I$ (i.e., optimizing $\mathbf{w}$ and $\mathbf{s}_{1(2)}$ in P1 using AO1 by assuming $\mathbf{H}_I = \mathbf{0}$). Based on the averaged result, we note that our proposed AO1 and AO2 algorithms for the double IRS design achieve very close performance with only 10^{-3} to 10^{-2} difference throughout P, and both are better than the rest benchmark schemes. The main reason is that the double IRS design with I-SSR provides new path for the signal transmission than single IRS case, and using the proposed algorithms, the reflected signals through the path Alice-IRS1-Bob (Eve), Alice-IRS2-Bob (Eve) and Alice-IRS1-IRS2-Bob (Eve) can be constructively (destructively) added at Bob (Eve), thereby providing more gain of SR. This indicates that the double IRS design with signal cooperation between IRS via the I-SSR channel greatly influences the SR performance.

[4]Note that the solution of PSCs by PRM algorithm is only a Riemmanian zero gradient point, not necessarily a KKT point solution. Hence, we state that the PRM based AO converges to a limit point solution.

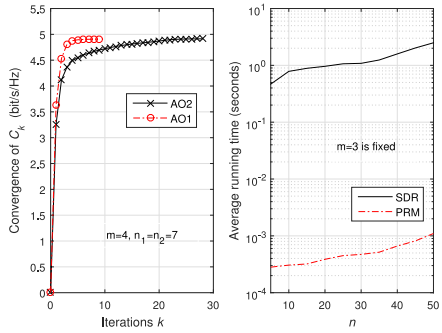

Fig. 3. Convergence of C_k versus k in P1 returned by proposed AO1 and AO2 algorithms, as well as the running time of the proposed SDR method for optimizing $\mathbf{s}_1$, $\mathbf{s}_2$ alternatively and PRM algorithm for optimizing $\mathbf{s}_1$, $\mathbf{s}_2$ simultaneously given $\mathbf{w}$. The results in the left figure are obtained via single randomly generated channels, and the ones in the right figure are averaged over 500 random channel realizations by fixing m and varying $n = n_1 = n_2$. The code of SDR and PRM are running in the same hardware and software environment.

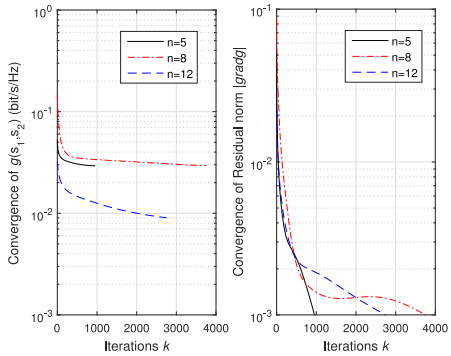

Fig. 4. Convergence of $g(\mathbf{s}_{1,k}, \mathbf{s}_{2,k})$ and the corresponding residual norm $|gradg| = |[grad_{\mathbf{s}_{1,k}} g^T, grad_{\mathbf{s}_{2,k}} g^T]^T|$ versus k via PRM algorithm. $m = 4$ and $n = n_1 = n_2$ is varying.

Fig. 3 illustrates the convergence of the value of objective function C_k in P1 versus k via proposed AO1 and AO2 algorithms as well as the running time of SDR method and PRM algorithm for optimizing $\mathbf{s}_1$ and $\mathbf{s}_2$ given $\mathbf{w}$ in one iteration of AO1 and AO2 algorithms. Note that in the left figure, both algorithms have monotonic convergence, and AO1 achieves much faster convergence (with only 9 iterations) than AO2 (with 28 iterations) given same initial point and target accuracy. In addition to this proposed results, based on our other extensive simulations, AO1 have faster convergence in most channel realizations. Even when AO1 converges slower than AO2 occasionally, the running speed of AO1 is significantly faster than AO2. This can be validated in

the right figure, in which given $\mathbf{w}$, the lower complexity PRM algorithm requires significantly shorter average time to compute $\mathbf{s}_1$ and $\mathbf{s}_2$ than that via SDR.

Fig. 4 shows the convergence of objective function $g(\mathbf{s}_{1,k}, \mathbf{s}_{2,k})$ in P3 and the corresponding residual norm of Riemannian gradient $|gradg| = |[grad_{\mathbf{s}_{1,k}} g^T, grad_{\mathbf{s}_{2,k}} g^T]^T|$ versus k via PRM algorithm under different channel realizations. Observe that $|gradg|$ gradually converges to $\epsilon_1 = 10^{-3}$ under all channel realizations. Although the convergence is not monotonic sometimes (see the curve when $n = 8$ in the right figure), the value of $g(\mathbf{s}_{1,k}, \mathbf{s}_{2,k})$ in the left figure is guaranteed to monotonically decreasing. Here we remark that although it takes large number of iterations (around hundreds and thousands) to reach convergence, the running speed of the whole process is fast due to low computational complexity.

V. Conclusion

In this correspondence, we consider a double IRS assisted secure wireless transmission model with I-SSR. To enhance the secrecy rate at Bob, we propose AO algorithm to jointly optimize the BF at transmitter and PSCs at IRS. In particular, during each iteration of AO, PRM algorithm is proposed to optimize the PCSs given BF. Simulation results have been shown to validate the performance and convergence of the proposed algorithms.

References

[1] H. Hasluda, Y. Kawamoto, and N. Kato, "Intelligent reflecting surface placement optimization in air-ground communication networks," *IEEE Wireless Commun.*, vol. 27, no. 6, pp. 146–151, Dec. 2020.

[2] H. Zhang, B. Di, L. Song, and Z. Han, "Reconfigurable intelligent surfaces assisted communications with limited phase shifts: How many phase shifts are enough?," *IEEE Trans. Veh. Technol.*, vol. 69, no. 4, pp. 4498–4502, Apr. 2020.

[3] B. Di *et al.*, "Hybrid beamforming for reconfigurable intelligent surface based multi-user communications: Achievable rates with limited discrete phase shifts," *IEEE J. Sel. Areas Commun.*, vol. 38, no. 8, pp. 1809–1822, Aug. 2020.

[4] M. Cui, G. Zhang, and R. Zhang, "Secure wireless communication via intelligent reflecting surface," *IEEE Wireless Commun. Lett.*, vol. 8, no. 5, pp. 1410–1414, Oct. 2019.

[5] H. Shen, W. Xu, S. Gong, Z. He, and C. Zhao, "Secrecy rate maximization for intelligent reflecting surface assisted multi-antenna communications," *IEEE Commun. Lett.*, vol. 23, no. 9, pp. 1488–1492, Sep. 2019.

[6] H.-M. Wang, J. Bai, and L. Dong, "Intelligent reflecting surface assisted secure transmission without eavesdropper's CSI," *IEEE Signal Process. Lett.*, vol. 27, pp. 1300–1304, Jul.. 2020.

[7] L. Dong and H.-M. Wang, "Secure MIMO transmission via intelligent reflecting surface," *IEEE Wirel. Commun. Lett.*, vol. 9, no. 6, pp. 787–790, Jun. 2020.

[8] L. Dong and H.-M. Wang, "Enhancing secure MIMO transmission via intelligent reflecting surface," *IEEE Trans. Wireless Commun.*, vol. 19, no. 11, pp. 7543–7556, Nov. 2020.

[9] B. Zheng, C. You, and R. Zhang, "Double-IRS assisted multi-user MIMO: Cooperative passive beamforming design," *IEEE Trans. Wireless Commun.*, to be published, doi: 10.1109/TWC.2021.3059945.

[10] J. Li, L. Zhang, K. Xue, and Y. Fang, "Secure transmission by leveraging multiple intelligent reflecting surfaces in MISO systems," 2020, *arXiv: 2008.03767*.

[11] X. Yu, D. Xu, Y. Sun, D. W. K. Ng, and R. Schober, "Robust and secure wireless communications via intelligent reflecting surfaces," *IEEE J. Sel. Areas Commun.*, vol. 38, no. 11, pp. 2637–2652, Nov. 2020.

[12] B. Zheng, C. You, and R. Zhang,"Efficient channel estimation for double-IRS aided multi-user MIMO system," 2020, *arXiv: 2011.00738*.

[13] P. Cao, J. Thompson, and H. V. Poor, "A sequential constraint relaxation algorithm for rank-one constrained problems," in *Proc. 25th Eur. Signal Process. Conf.*, Kosovo, 2017, pp. 1060–1064.

[14] P.-A. Absil, R. Mahony, and R. Sepulchre, *Optimization Algorithms on Matrix Manifolds*. Princeton, NJ, USA: Princeton Univ. Press, 2009.

[15] N. Boumal, P.-A. Absil, and C. Cartis,"Global rates of convergence for nonconvex optimization on manifolds," *IMA J. Numer. Anal.*, vol. 39, no. 1, pp. 1–33, 2018.